Progress In Electromagnetics Research Letters, Vol. 88, 43–50, 2020

A Novel Dual-Frequency Omnidirectional Antenna with Transmission Line Resonators Loading

Honglin Zhang[1], Dong Chen[1, *], Ying Yu[1], and Chunlan Zhao[2]

Abstract—A novel dual-frequency antenna with horizontally polarized (HP) omnidirectional radiation is presented in this paper. The antenna consists of four printed arched dipoles, four planar baluns, and a four-way power splitter. The balun as well as the power splitter works as the feed network. By loading a transmission line resonator (TLR) as the near-field coupling parasitic element, the dual-frequency characteristics can be realized. After the design principle is stated, a sample antenna is manufactured and measured to prove the predicted performance of the proposed antenna. The measured results agree well with the predicted ones.

1. INTRODUCTION

The horizontal polarization (HP) omnidirectional antenna is widely used in mobile terminals or base station, which can uniformly transmit or receive HP wireless signals from any directions on the azimuth plane to improve the coverage of the space. With the rapid development of wireless communication system, HP omnidirectional antenna plays an increasingly important role in communication systems.

In theory, a magnetic dipole has HP omnidirectional radiation; however, the magnetic dipole is unavailable in reality. A loop antenna with a uniform current distribution has an omnidirectional pattern, and the wire-structure Alford loop is initially reported to realize the omnidirectional pattern with HP [1]. From then on, several similar Alford loop antennas have been extensively studied [2–5]. Recently, some novel loop antennas have been introduced in [6, 7]. However, a loop antenna has the disadvantages of small radiation resistance and high reactance, which lead to poor impedance matching and narrow bandwidth [8]. Moreover, HP omnidirectional pattern can also be realized by antenna arrays [9]. Many HP omnidirectional antennas based on the rotational dipole arrays are proposed in [10–16]; however, such proposed antennas work at single-frequency.

In this paper, a dual-frequency HP omnidirectional antenna is proposed, which consists of a rotational dipole array and an integrated planar balun working as the feeding network. Four printed dipole antennas are placed vertically to each other on the substrate to realize HP omnidirectional radiation. To obtain better omnidirectional radiation performance, each printed dipole is designed to be arched along the boundary of the disk-shaped substrate. Based on the principle of near-field coupled parasitic element [17], dual-frequency performance can be achieved by loading a transmission line resonator (TLR). After the design method is analyzed, a sample antenna is fabricated and measured. The measurement is in good agreement with the predicted results, which verifies our design method.

Received 12 September 2019, Accepted 19 November 2019, Scheduled 6 December 2019

* Corresponding author: Dong Chen (chendong@njupt.edu.cn).

[1] College of Electronic and Optical Engineering & College of Microelectronics, Nanjing University of Posts and Telecommunications, No. 66, Xinmofan Road, Nanjing 210003, China. [2] 13th Research Institute, China Electronic Technology Group Corporation, No. 113, Hezuo Road, Shijiazhuang 050051, China.

2. ANTENNA AND ITS EQUIVALENT CIRCUIT

Figure 1 depicts the structure of the proposed antenna. Because of the flexible characteristic and low loss factor over a wide frequency range [18], polyimide (PI) is chosen as the substrate in our design. The proposed antenna is implemented on a PI substrate with a thickness 0.065 mm, dielectric constant $\varepsilon_r = 3.5$, and loss tangent $\delta = 0.0027$, respectively. The feed matching network is constructed by four planar baluns and a four-way power splitter. The four arched printed dipole elements are etched on one side of the substrate, while the baluns as well as the power splitter is built on the other side.

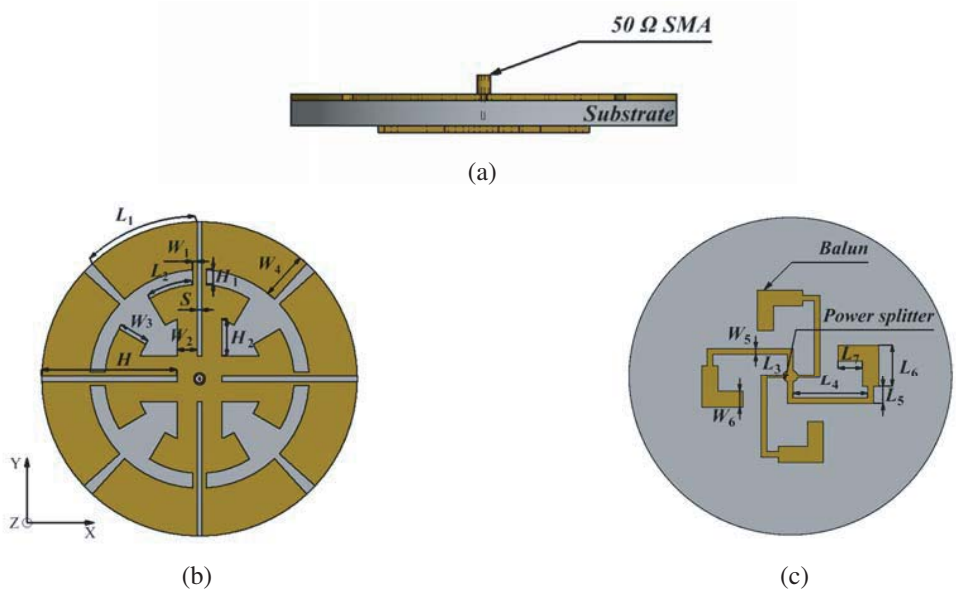

Figure 1. Configuration of the proposed HP omnidirectional antenna: (a) Side view; (b) Top view; (c) Bottom view.

Since the HP omnidirectional antenna is composed of four identical arched dipoles, a quarter of this antenna and its equivalent circuit are illustrated in Figs. 2(a) and (b), respectively [19]. The printed dipole is fed by a slot line (i.e., slot line in Fig. 2(a)).

The input impedance of the printed dipole is denoted by Z_{ra}. The impedance looking into the slot line (the characteristic impedance is Z_4, and the length of the slot line is l_4, respectively) is Z_r. Z_c is the impedance looking into the loaded TLR. Impedance Z_b is obtained by connecting impedance Z_c in parallel with the shorted stub (the characteristic impedance is Z_3, and the length of the slot line is l_3, respectively). The coupling between slot line and microstrip line can be expressed as an ideal transformer with turn ratio n [20]. By the transformer, impedance Z_b is converted to Z_a. Z_{in} is obtained by considering the open stub (the characteristic impedance is Z_2, and the length of the microstrip line is l_2, respectively). Ultimately, the input impedance looking into the microstrip line (the characteristic impedance is Z_1, and the length of the slot line is l_1, respectively) at the feed point is Z'_{in}.

Next, a mathematical derivation of the equivalent circuit in Fig. 2 is performed. Based on the discussion above, the input impedance Z_{ra} of the printed dipole can be obtained by CST EM simulation software. From the impedance equation of the transmission line, impedance Z_r can be established

$$Z_r = Z_4 \frac{Z_{ra} + jZ_4 \tan \beta_4 l_4}{Z_4 + jZ_{ra} \tan \beta_4 l_4} \tag{1}$$

where using the empirical formula [21], parameters Z_4 and β_4 (phase constant of the slot line) can be calculated.

As can be seen from Fig. 2, impedance Z_b of the antenna can be established

$$\frac{1}{Z_c} = \frac{1}{Z_r} + \frac{1}{j\omega L} + j\omega C \tag{2}$$

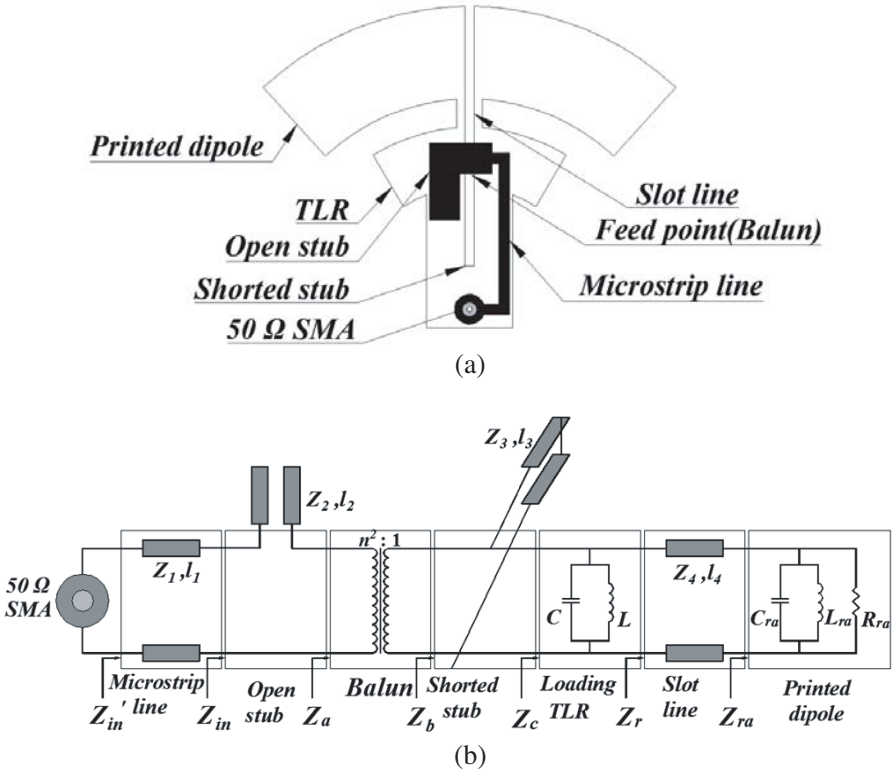

Figure 2. Evolution of the proposed antenna: (a) The quarter section of the proposed antenna; (b) The equivalent circuit ($l_1 = L_3 + L_4 + L_5$, $l_2 = L_6 + L_7$, $l_3 = H_2$, $l_4 = H_1$).

where L and C can be calculated by the empirical formulas in [22, 23]. Thus, impedance Z_b can also be established

$$Z_b = \frac{jZ_cZ_3 \tan \beta_4 l_3}{Z_c + jZ_3 \tan \beta_4 l_3} \tag{3}$$

Similarly, impedance Z_3 can be calculated by empirical formulas [21]. After passing through the transformer, impedance Z_a is transformed to Z_b.

$$Z_a = n^2 Z_b \tag{4}$$

Considering the open stub, Z_{in} can be obtained

$$Z_{in} = Z_a - jZ_2 \cot \beta_2 l_2 \tag{5}$$

where β_2 is the phase constant of the microstrip line.

Ultimately, the input impedance can be obtained

$$Z'_{in} = Z_1 \frac{Z_{in} + jZ_1 \tan \beta_2 l_1}{Z_1 + jZ_{in} \tan \beta_2 l_1} \tag{6}$$

Then, Z_{in} in the equation can be derived as

$$Z_{in} = Z_1 \frac{Z'_{in} - jZ_1 \tan \beta_2 l_1}{Z_1 - jZ'_{in} \tan \beta_2 l_1} \tag{7}$$

However, Z'_{in} is extracted by CST EM simulation software. Therefore, impedance Z_{in} can be determined from Equation (7).

So far, the equivalent circuit has been deduced, and full-wave simulation will be used to analyze our design.

An investigation about the effect on the resonant frequency of the antenna caused by different arc lengths L_2 is carried out by CST 3D EM simulation software. Under simulation, the other size parameters are set as follows: $L_1 = 11.0\,\text{mm}$, $L_3 = 2.2\,\text{mm}$, $L_4 = 6.9\,\text{mm}$, $L_5 = 1.6\,\text{mm}$, $L_6 = 4.2\,\text{mm}$, $L_7 = 2.3\,\text{mm}$, $W_1 = 0.4\,\text{mm}$, $W_2 = 1.9\,\text{mm}$, $W_3 = 3.0\,\text{mm}$, $W_4 = 4.6\,\text{mm}$, $W_5 = 0.5\,\text{mm}$, $W_6 = 1.5\,\text{mm}$, $H = 12.9\,\text{mm}$, $H_1 = 1.4\,\text{mm}$, $S = 0.4\,\text{mm}$ and $H_2 = 3.5\,\text{mm}$.

Simulated S-parameters of the proposed antenna with different L_2 as well as that of a conventional printed dipole without TLR are simultaneously plotted in Fig. 3. As can be seen from Fig. 3, dual-frequency characteristics can be observed by loading a TLR, and the second resonant frequency continuously moves to the lower frequency band with the increase of L_2, while the first resonant frequency keeps almost the same, which means that the two resonant frequencies can be adjusted independently.

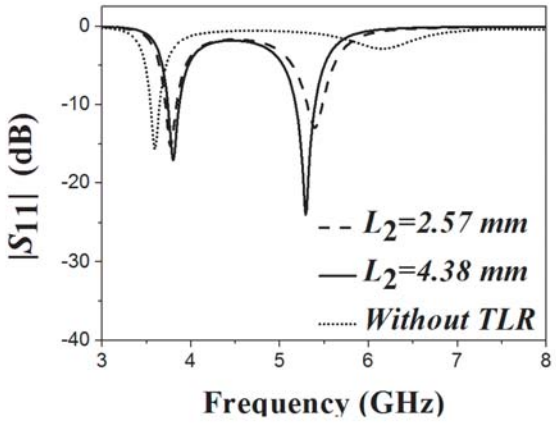

Figure 3. The simulated S_{11} varies with L_2.

3. MEASURED RESULTS

To verify our design, a sample antenna is fabricated and measured. The size parameters of the sample antenna are optimized as follows: $L_1 = 11.0\,\text{mm}$, $L_2 = 4.4\,\text{mm}$, $L_3 = 2.2\,\text{mm}$, $L_4 = 6.9\,\text{mm}$, $L_5 = 1.6\,\text{mm}$, $L_6 = 4.2\,\text{mm}$, $L_7 = 2.3\,\text{mm}$, $W_1 = 0.4\,\text{mm}$, $W_2 = 1.9\,\text{mm}$, $W_3 = 3.0\,\text{mm}$, $W_4 = 4.6\,\text{mm}$, $W_5 = 0.5\,\text{mm}$, $W_6 = 1.5\,\text{mm}$, $H = 12.9\,\text{mm}$, $H_1 = 1.4\,\text{mm}$, $S = 0.4\,\text{mm}$ and $H_2 = 3.5\,\text{mm}$. A photograph of the fabricated antenna is shown in Fig. 4. The return loss and radiation pattern have been measured by Kegsight E5071C vector network analyzer and SATIMO near-field antenna measurement system, respectively.

The simulated and measured S-parameters are both shown in Fig. 5. There are some deviation between the simulation and measurement, which might be caused by the fabrication tolerance. However, the dual-frequency resonant characteristics of this antenna can be observed obviously.

The measured and simulated radiation patters on E-plane and H-plane at 3.8 GHz and 5.3 GHz are plotted in Fig. 6 and Fig. 7, respectively.

From Fig. 6 and Fig. 7, it can be seen that the horizontal radiation pattern is omnidirectional, and the cross-polarization level is less than $-23\,\text{dB}$. There are some deviation between the simulation and measurement, which might be caused by SMA welding precision and dielectric constant variation of the substrate.

Simultaneously, Fig. 8 depicts measured radiation efficiency and gain of the proposed antenna over the operating frequency range. As can be seen from Fig. 8(a), there are two peaks on the measured radiation efficiency curve, 91% and 78%, respectively. Similarly, in Fig. 8(b), there are two gain peaks, 1.69 dBi and 1.02 dBi, respectively. It should be noted that the radiation efficiency and gain tend to be lower at the high frequency. This may be due to the increase of metal loss at the higher frequency band. Likewise, the slight deviation between the simulation and measurement may also be caused by SMA welding precision and dielectric constant variation of the substrate.

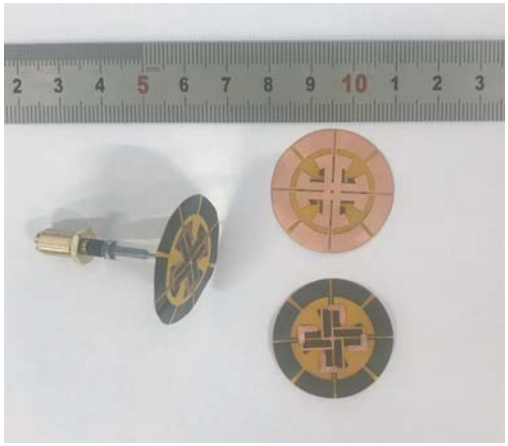

Figure 4. Photograph of the proposed HP omnidirectional antenna.

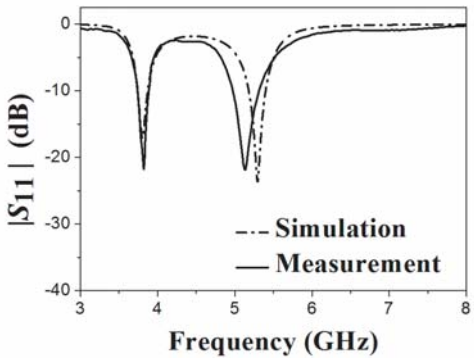

Figure 5. Simulated and measured return loss of the proposed HP omnidirectional antenna.

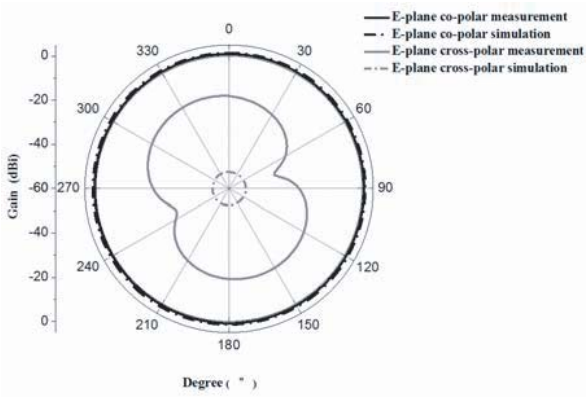

(a)

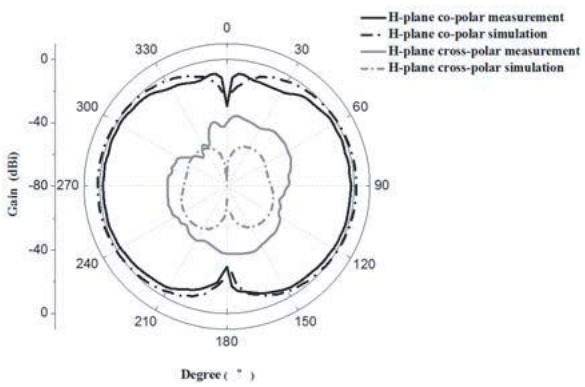

(b)

Figure 6. Simulated and measured radiation patterns of the proposed HP omnidirectional antenna at 3.8 GHz: (a) E-plane; (b) H-plane.

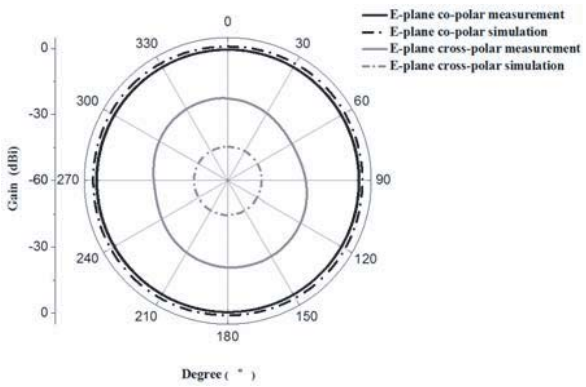

(a)

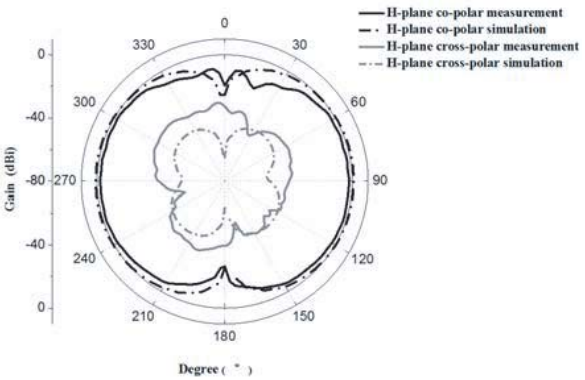

(b)

Figure 7. Simulated and measured radiation patterns of the proposed HP omnidirectional antenna at 5.3 GHz: (a) E-plane; (b) H-plane.

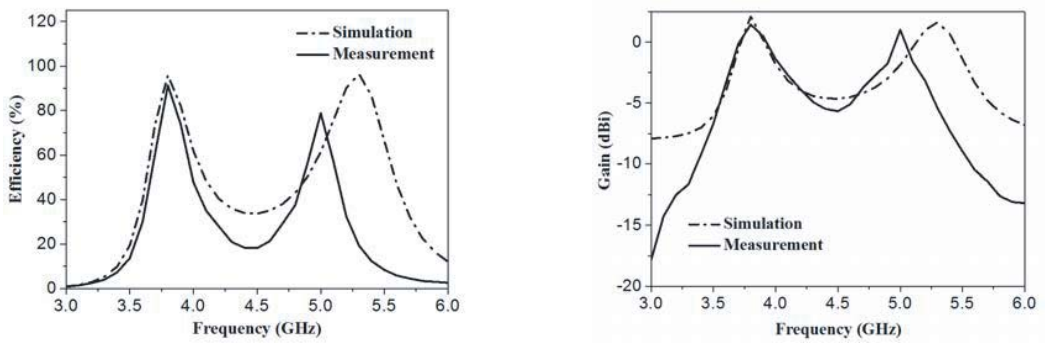

(a) (b)

Figure 8. Measured radiation efficiency and gain of the proposed HP omnidirectional antenna: (a) Radiation efficiency; (b) Gain.

The proposed HP omnidirectional antenna is also compared with the other published references in recent years in Table 1.

Table 1. Comparison of various dual-frequency HP omnidirectional antennas.

Reference Designs	Operating Freq. (GHz)	Substrate ε_r	Antenna size (mm^3)	Gain variation (dB)	X-pol (dB)
[24]	2.48 GHz & 5.43 GHz	Not mentioned	Not mentioned	0.5 @ 2.42 GHz & Not mentioned @ 5.43 GHz	−18
[25]	2.45 GHz & 3.9 GHz	2.2	47 × 47 × 1.57	1.7 @ 2.45 GHz & 1.2 @ 3.9 GHz	−20
[26]	2.4 GHz & 5.6 GHz	Not mentioned	20 × 25 × 16	0 @ 2.4 GHz & 0.6 @ 5.6 GHz	−11.3
[27]	0.89 GHz & 1.84 GHz	4.4	94 × 94 × 1	0.65 @ 0.89 GHz & 3.95 @ 1.84 GHz	−20
Proposed Antenna	3.8 GHz & 5.3 GHz	3.5	30 × 30 × 0.065	1.5 @ 3.8 GHz & 0.8 @ 5.3 GHz	−23

X-pol: Cross polarization

As can be seen from Table 1, the proposed antenna provides dual-frequency operation with a relatively reduced size. In addition, the proposed antenna has a better cross-polarization level and good gain variation. Compared with the planar structure of the proposed antenna, space installation is adopted in [24] and [26]; therefore, they are not compact. On the other hand, the proposed antenna is more compact than [25] by using a low-profile and a relatively high dielectric constant substrate. Therefore, the proposed antenna with compact structure has dual-frequency and good radiation characteristics.

4. CONCLUSION

In this paper, a novel dual-frequency HP omnidirectional antenna is presented. The dual-frequency characteristic is realized by loading a TLR which works as a near-field coupling parasitic element. To realize the HP omnidirectional radiation pattern, four identical arched dipole antennas are arranged along the circumference of the substrate to form a circular array. A prototype antenna has been fabricated and measured. The measurements agree well with the simulations. HP omnidirectional radiation pattern is realized at both working frequencies, which provide a good verification for our proposed design method.

ACKNOWLEDGMENT

This work is supported by the National Natural Science Foundation of China (NSFC) under project No. U1636108, the Key university science research project of Jiangsu Province project No. 17KJA470005, and SATIMO near-field antenna measurement system supplied by Nanjing University of Posts and Telecommunications.

REFERENCES

1. Alford, A., A. G. Kandoian, et al., "Ultrahigh-frequency loop antennas," *IEEE Trans. AIEE*, Vol. 56, No. 12, 843–844, Dec. 1940.
2. Lin, C.-C., L.-C. Kuo, H.-R., Chuang, et al., "A horizontally polarized omnidirectional printed antenna for WLAN applications," *IEEE Trans. Antennas Propag.*, Vol. 54, No. 11, 3551–3556, Nov. 2006.
3. Fenn, C., et al., "Arrays of horizontally-polarized loop-fed slotted cylinder antennas," *IEEE Trans. Antennas Propag.*, Vol. 33, No. 4, 375–382, Jan. 1985.
4. Li, W. W., K. W. Leung, et al., "Omnidirectional circularly polarized dielectric resonator antenna with TOP-loaded alford loop for pattern diversity design," *IEEE Trans. Antennas Propag.*, Vol. 61, No. 8, 4246–4256, 2007.
5. Kim, D. S., C. H. Ahn, Y. T. Im, S. J. Lee, K. C. Lee, W. S. Park, et al., "A windmill-shaped loop antenna for polarization diversity," *IEEE Trans. Antennas Propag. — Soc. Int. Symp.*, 361–364, Honoluu, HI, Jun. 2007.
6. Wei, K., Z. Zhang, Z. Feng, M. F. Iskander, et al., "A MNG-TL loop antenna array with horizontally polarized omnidirectional patterns," *IEEE Trans. Antennas Propag.*, Vol. 60, No. 6, 2702–2710, Apr. 2012.
7. Wei, K., Z. Zhang, Z. Feng, et al., "Design of a wideband horizontally polarized omnidirectional printed loop antenna," *IEEE Antennas Wireless Propag. Lett.*, Vol. 11, 49–52, Jan. 2012.
8. Balanis, C. A., *Antenna Theory: Analysis and Design*, 4th edition, Wiley-Interscience, Hoboken, NJ, USA, 2016.
9. Brachat, P. and C. Sabatier, "Wideband omnidirectional microstrip array," *Electron Lett.*, Vol. 37, No. 6, 2–3, Feb. 2016.
10. Cai, X. Z., K. Sabatier, et al., "A compact broadband horizontally polarized omnidirectional antenna using planar folded dipole elements," *IEEE Trans. Antennas Propag.*, Vol. 64, No. 2, 414–422, Feb. 2016.
11. Wang, Z. D., Y. Z. Yin, X. Ying, J. J. Wu, et al., "Design of a wideband horizontally polarized omnidirectional antenna with mutual coupling method," *IEEE Trans. Antennas Propag.*, Vol. 63, No. 7, 3311–3316, Jul. 2015.
12. Quan, X. L., R. L. Li, et al., "A broadband dual-polarized omnidirectional antenna for base stations," *IEEE Trans. Antennas Propag.*, Vol. 61, No. 2, 943–947, Feb. 2013.
13. Zhang, H. Y., Zhang, F. Zhang, T. Li, C. Li, et al., "Bandwidth enhancement of a horizontally polarized omnidirectional antenna by adding parasitic strips," *IEEE Trans. Antennas Propag.*, Vol. 16, 880–883, Sep. 2017.
14. Fan, K., Z. C. Hao, J. Yuan, G. Q. Hu, W. Hong, et al., "Wideband horizontally polarized omnidirectional antenna with a conical beam for millimeter-wave applications," *IEEE Trans. Antennas Propag.*, Vol. 66, No. 9, 4437–4448, Jun. 2018.
15. Liu, Y., J. Xue, H. Wang, S. Gong, et al., "Low-profile omnidirectional dual-polarised antenna for 2.4 GHz WLAN applications," *Electron Lett.*, Vol. 50, No. 14, 975–976, Jul. 2014.
16. Huang, H., Y. Liu, Gong, et al., "Broadband dual-polarized omnidirectional antenna for 2G/3G/LTE/WiFi applications," *IEEE Antennas Wireless Propag. Lett.*, Vol. 15, 576–579, Jul. 2015.
17. Ziolkwski, R. W., P. Jin, C. C. Lin, et al., "Metamaterial-inspired engineering of antennas," *Proc. IEEE*, Vol. 99, No. 10, 1720–1731, Oct. 2011.

18. Khaleel, H. R., H. M. Al-Rizzo, D. G. Rucker, S. M. Mohan, et al., "A compact polyimide-based UWB antenna for flexible electronics," *IEEE Antennas Wireless Propag. Lett.*, Vol. 11, 564–567, May 2012.
19. Li, R. L., T. Wu, B. Pan, K. Lim, J. Laskar, M. M. Tentzeris, et al., "Equivalent-circuit analysis of a broadband printed dipole with adjusted integrated balun and an array for base station applications," *IEEE Trans. Antennas Propag.*, Vol. 57, No. 7, 2180–2184, May 2009.
20. Gupta, K. C., R. Garg, I. Bahl, and P. Bhartia, *Microstrip Line and Slotlines*, 2th edition, Artech House, London, Boston, USA, 2016.
21. Janaswamy, R., D. H. Schaubert, et al., "Characteristic impedance of a wide slotline on low-permittivity substrates," *IEEE Trans. Microw. Theory Tech.*, Vol. 34, No. 8, 900–902, Aug. 1986.
22. Pozar, D. M., *Microwave Engineeing*, 4th edition, John Wiley & Sons, New York, USA, 2011.
23. Makimoto, M. and S. Yamashita, *Microwave Resonators and Filters for Wireless Communication: Theory, Design and Application*, Springer, Berlin, Germany, 2001.
24. Luo, P., Y. Cui, R. Li, et al., "Novel multiband/broadband horizontally polarized omnidirectional antennas," *IEEE International Symposium on Antennas and Propagation (APSURSI) 2016*, Jul. 2016.
25. Ahn, C.-H., S.-W. Oh, K. Chang, et al., "A dual-frequency omnidirectional antenna for polarization diversity of MIMO and wireless communication applications," *IEEE Antennas Wireless Propag. Lett.*, Vol. 8, 966–969, Aug. 2009.
26. Ando, A., N. Kita, W. Yamada, et al., "2.4/5-GHz dual-band vertically/horizontally dual-polarized omnidirectional antennas for WLAN base station," *IEEE Antennas and Propagation Society International Symposium 2008*, Jul. 2008.
27. Lai, J., B. Feng, Q. Zeng, S. Su, et al., "A dual-band dual-polarized omnidirectional antenna for 2G/3G/LTE indoor system applications," *IEEE International Conference on Signal Processing, Communications and Computing (ICSPCC) 2018*, Sep. 2018.